mer Fellowship at the Kent State University.

†Based in part on masters theses submitted by AD and RFK to the Department of Physics, Kent State University.

[1]W. R. Johnson and C. J. Mullin, Phys. Rev. 119, 1270 (1960).

[2]V. G. Gorshkov and A. I. Mikhailov, Zh. Eksperim. i Teor. Fiz. 44, 2142 (1963) [Soviet Phys. JETP 17, 1439 (1963)].

[3]V. G. Gorshkov, A. I. Mikhailov, and V. S. Polikanov, Nucl. Phys. 55, 273 (1964).

[4]J. C. Jaeger and H. R. Hulme, Proc. Cambridge Phil. Soc. 32, 158 (1936).

[5]W. R. Johnson, D. J. Buss, and C. O. Carroll, Phys. Rev. 135, A1232 (1964).

[6]W. R. Johnson, Phys. Rev. 159, 61 (1967).

[7]C. V. Sheth and N. V. V. J. Swamy, Phys. Rev. 167, 319 (1968).

[8]C. O. Carroll and R. F. O'Connell, Phys. Rev. 132, 2540 (1963).

[9]For example, W. Heitler, *Quantum Theory of Radiation* (Oxford U.P., Oxford, 1954), 3rd ed., p. 143.

[10]For example, M. E. Rose, *Relativistic Electron Theory* (Wiley, New York, 1961), p. 172.

[11]G. K. Horton and E. Phibbs, Phys. Rev. 96, 1066 (1954).

[12]For example, W. Grobner and N. Hofreiter, *Integraltafel, Zweiter Teil, Bestimmte Integrale* (Springer-Verlag, Wien and Innsbruck, 1958), Zweite, verbessert Auflage, p. 2.

[13]A. Davidz, M. A. thesis, Kent State University, 1965 (unpublished).

[14]R. F. Kess, M. A. thesis, Kent State University, 1966 (unpublished).

PHYSICAL REVIEW A VOLUME 1, NUMBER 6 JUNE 1970

# Hyperfine Interaction Induced by Electron Capture. I. $\gamma$-$\gamma$ Directional-Correlation Experiments*†

H. J. Leisi

*Bartol Research Foundation of the Franklin Institute, Swarthmore, Pennsylvania* 19081

*and*

*Laboratory for High Energy Physics, Swiss Federal Institute of Technology, Zürich, Switzerland*‡

(Received 21 November 1969)

$\gamma$-$\gamma$ directional-correlation experiments performed on low-density gaseous sources of xenon isotopes are described. The angular correlations corresponding to the cascade transitions of 172–203 keV in $^{127}$I and 55–188 keV in $^{125}$I have been measured and found to be strongly perturbed. The effect is ascribed to the hyperfine interaction of the iodine ions that are formed following $K$ capture of xenon isotopes. An interference phenomenon that results in the appearance of a resonance in the coincidence counting rate has been observed for the $\gamma$-$\gamma$ cascade of 172–203 keV. The effect is interpreted as being due to the crossing of hyperfine energy levels at zero magnetic field.

## I. INTRODUCTION

A large number of experiments have been performed to investigate so-called "after effects", i.e., perturbations of angular correlations or effects on Mössbauer spectra due to preceding decay processes.[1] A vigorous discussion on after effects in angular correlations, held at the Uppsala meeting,[2] revealed the desirability for more clear-cut experiments to investigate these phenomena.

In the present paper, we describe experiments designed to study effects on $\gamma$-$\gamma$ angular correlations of preceding $K$-capture decays. All previous work concerned with this problem has been done with solid sources of various kinds. Under these circumstances, it is often difficult to separate unambiguous perturbations due to $K$ capture from those existing in the solid. In order to study pure $K$-capture effects, we have used monoatomic gaseous sources at low densities. At sufficiently low gas pressure, the extranuclear fields affecting the correlation are solely provided by the decaying atom itself and are free from influence of the environment. Although the results of such a study cannot immediately be applied to the situation in a solid, an investigation of the "simple" case of a free decaying atom appears to be the first step toward a clear understanding of after effects.

The present work has also been undertaken in order to search for characteristic effects in perturbed angular correlations associated with a time-independent hyperfine interaction. According to theoretical predictions,[3] a resonance should occur in an angular correlation when measured as a function of a weak externally applied magnetic field. It was felt that in a gaseous source at low

density the conditions for the appearance of a resonance could possibly be realized.

In Sec. II, we describe in some detail the gas purification system that has been used to prepare the $^{127}$Xe sources. This technique may be employed for preparing low-density sources of any rare-gas isotope. Section III contains the angular correlation measurements of the present work together with a compilation of all presently known anisotropy values of angular correlations that were obtained from low-density gaseous sources of $^{127}$Xe and $^{125}$Xe. The resonance experiment is described in Sec. IV.

## II. SOURCE PREPARATIONS

### A. Xenon 127

The $^{127}$Xe activity was prepared by irradiating KI with protons in the 86-in. cyclotron at the Oak Ridge National Laboratory according to the reaction $^{127}$I $(p,n)$ $^{127}$Xe. The target material was packed in a vacuum-tight nickel tube. After the irradiation, the active xenon could be extracted by heating the target above the melting point of KI(723 °C). The main problem in preparing the $^{127}$Xe sources was the purification of xenon from other gases which also escaped from the target at the elevated temperature. This was achieved with the aid of the purification system shown schematically in Fig. 1. The essential part is the calcium furnace which serves to produce Ca vapor in a closed system containing the small amount of xenon together with the other gases. One makes use of the property of Ca vapor to form solid compounds with all except the inert gases.[4] With this technique, it was possible to remove (quantitatively) amounts of foreign gas corresponding to pressures up to a few tens of Torr in the apparatus of Fig. 1 (volume approximatively 250 cm$^3$).

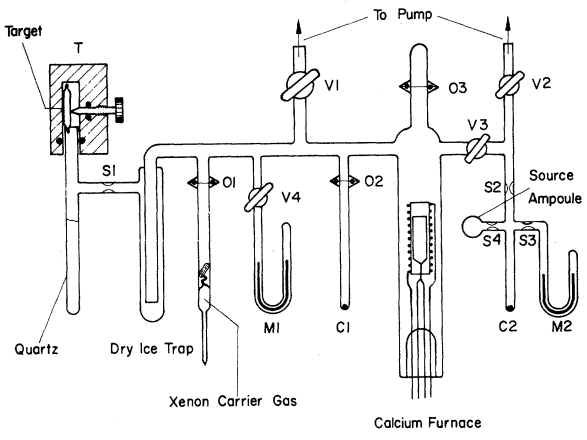


FIG. 1. Purification system for preparing low-density rare-gas sources (schematic). The system was used to obtain the $^{127}$Xe sources.

A typical source preparation proceeded as follows. The irradiated target was placed in the metallic target opener $T$ (see Fig. 1). Before opening the target, the whole system was connected to an oil diffusion pump equipped with a liquid-nitrogen cold trap. During this outgasing period, the charcoal traps C1 and C2, which served to transfer the gaseous xenon from one section of the apparatus to another, had to be held at a temperature of about 300 °C. The Ca furnace containing metallic calcium was also operated at about the same temperature. The target section of the system was then isolated by closing the valves V3 and V1. Xenon carrier gas (see Fig. 1) was released by opening the brake seal. A hole was then drilled in the target by means of a metallic needle (see Fig. 1 ). The $^{127}$Xe activity was extracted by letting the target drop into a quartz section of the apparatus and heating this section above the melting point of KI. When activity measurements on the target indicated complete escape of $^{127}$Xe, the whole section comprising target opener and quartz oven was removed from the system by closing the glass tube at the seal-off place S1. The purification process proper was started by closing valve V4 and raising the temperature in the Ca-furnace. At temperatures between 450 and 600 °C, a black Ca mirror in the upper parts of the Ca furnace indicated a strong formation of Ca vapor. The evaporation was maintained over a period of 15 min. Then the source section of the system was disconnected from the pump by closing V2. The small oven providing a temperature of 300 °C at the charcoal trap C2 was replaced by a liquid-nitrogen Dewar and the valve V3 was opened. The trap C2 was held at liquid-nitrogen temperature for 10 min in order to solidify and thereby collect xenon gas from the whole system. After this period, the valve V3 was closed and the source section containing the xenon activity was separated from the system at the seal-off place S2. The total gas pressure in the source section was measured with the mercury manometer M2 while the temperature of the charcoal trap C2 was again 300 °C. Then the manometer was removed at S3 and source ampoule and charcoal trap were finally separated at the seal off place S4. The yield of the source preparation by this technique was essentially given by the ratio of the volumes of source ampoule and total source section (below S2). By using glass tubing of small internal diameters in the source section, total yields of 90% were realized.

All valves and all "O"-ring seals (01, 02, 03) of the purification system were greaseless in order to prevent loss of xenon activity and contamination of the system. Construction details of the

Ca furnace are shown in Fig. 2. The heating element of the furnace consisted of about 50 turns of tantalum wire (diam 20 mil).

### B. Xenon 125

The $^{125}$Xe activity was obtained by irradiating natural xenon gas at the research reactor of the Oak Ridge National Laboratory. A quartz ampoule (volume of 1.2 cm$^3$) was filled with xenon at a pressure of 2.7 Torr and irradiated for 24 h at a flux of $2\times10^{14}$ $n/\text{cm}^2$ sec. In order to avoid interference with the activity produced in the quartz, the ampoule was broken under vacuum with the device shown in Fig. 3. The xenon activity was isolated from the quartz splinters by cooling the source ampoule (see Fig. 3) with liquid nitrogen and separating the two parts of the system at the seal-off point S1. The total pressure at room temperature in the source section was measured with the Hg manometer. The manometer was then disconnected at S2 while the source ampoule was again immersed in liquid nitrogen, and finally, the source ampoule was sealed off at S3, the remaining part of the system being at room temperature.

## III. ANISOTROPY MEASUREMENTS WITHOUT MAGNETIC FIELD

All the measurements reported in this paper were performed with the fast-slow coincidence system described earlier.[5] Harshaw integral-line NaI (TI) detectors with dimensions 3 in. diam $\times$3 in. height and 2 in. diam$\times$2 in. height were used for the anisotropy measurements described in this section.

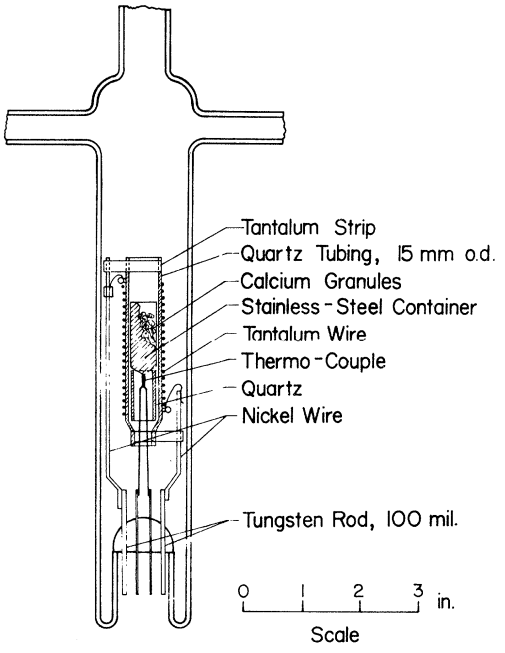


FIG. 2. Calcium furnace of gas purification system.

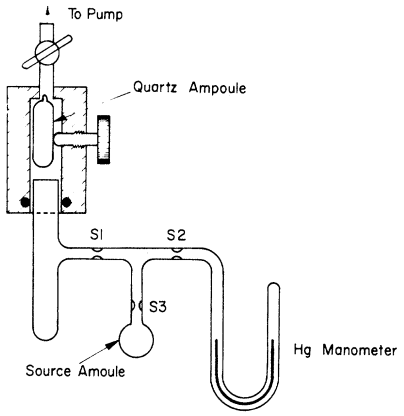


FIG. 3. System for preparing the source of $^{125}$Xe (schematic). The total volume was approximatively 40 cm$^3$.

### A. 172–203 keV Angular Correlation in $^{127}$I

A $^{127}$Xe source in a spherical pyrex ampoule of 13 mm o.d. and a wall thickness of about $\frac{1}{2}$ mm was prepared following the procedure described in Sec. II A. A total gas pressure of 2±1 Torr was measured which comprises a xenon carrier gas pressure of 0.5 Torr. The 2×2-in. detector was used as the movable detector to measure the 203-keV $\gamma$ ray, at a distance of 2 in. from the source. The 3×3-in. detector was placed at 0°, at a distance of 3 in. from the source. Lead absorbers of 0.32 and 0.52 g/cm$^2$, respectively, were placed in front of the detectors in order to reduce crystal-to-crystal scattering in the 180° position of the 375-keV cross-over $\gamma$ ray. The same effect was suppressed in the 90° position by placing a Pb plate of thickness $\frac{1}{8}$ in. at the 45° position. An uncorrected anisotropy value of $A' = 0.073 \pm 0.006$ was obtained. Correcting the effects of both finite solid angles according to the tables of Yates[6] and finite source extension according to formula (3) of Ref. 5, we find the anisotropy value given in Table I.[7]

### B. 55–188 keV Angular Correlation in $^{125}$I

A $^{125}$Xe source in a spherical glass ampoule of 20 mm o.d. and wall thickness approximatively $\frac{1}{2}$ mm was prepared as described in Sec. II B. A total gas pressure of 3±1 Torr was found, which includes air and 0.6 Torr of xenon. The source intensity was measured to be 30 $\mu$Ci 24 h after

TABLE I. Anisotropies of $\gamma$-$\gamma$ directional correlations in gaseous sources at low pressure.

| Isotope | Cascade (energies in keV) | Gas pressure (Torr) | Anisotropy $A = \frac{W(\pi) - W(\frac{1}{2}\pi)}{W(\frac{1}{2}\pi)}$ Gaseous source | Metallic source | Unperturbed correlation |
|---|---|---|---|---|---|
| $^{127}$I | 172–203 | 2±1 | 0.099 ±0.008 this work | 0.377±0.007 (Ref. 5) | |
| | | ~1 | 0.05 ±0.03 (Ref. 9) | | |
| | | 0.78±0.25 | 0.1062±0.0035 (Ref. 8) | | |
| $^{125}$I | 55–188 | 3±1 | 0.11 ±0.02 this work | 0.400±0.024[a] | |
| | | 2±1 | 0.089 ±0.005[b] | | |
| $^{127}$I | 145–58 | 1.6 ±0.6 | −0.09 ±0.05 (Ref. 5) | | −0.305±0.007 (Ref. 5) |
| | | 0.78±0.25 | −0.065 ±0.020 (Ref. 10) | | |

[a]J. S. Geiger, Phys. Rev. 158, 1094 (1967).

[b]Th. v. Ledebur, F. N. Gygax, and H. J. Leisi, Helv. Phys. Acta 42, 581 (1969).

the end of the irradiation. The 55-keV $\gamma$ ray was measured with the fixed 3×3-in. detector at a distance of 8 in. from the source. The source detector distance of the movable 2×2-in. detector was 3 in. Both detectors were equipped with a lead cylinder (wall thickness $\frac{1}{8}$ in.) which served to reduce the room background. In order to prevent the $K$ x rays of lead from entering the 55-keV detector, a cadmium sheet of thickness $\frac{1}{16}$ in. was inserted between the lead mantle and the 3×3-in. detector. For the same purpose, a Cd sheet was also placed around the lead cylinder of the 2×2-in. detector. An iron sheet of thickness 0.33g/cm$^2$ in front of the 188-keV detector served to absorb the low-energy $\gamma$ rays, while the front face of the 55-keV detector was uncovered. Figure 4 shows the singles and coincidence spectra of the 3×3-in. detector in the vicinity of the 55-keV line, taken immediately after the anisotropy measurement (about 38 h after the end of the irradiation). The singles spectrum shows already the presence of the 81-keV $\gamma$ ray from the decay of $^{133}$Xe while the coincidence spectrum exhibits a clean line of 55 keV. We obtained an uncorrected anisotropy value of $A' = 0.096 \pm 0.010$. Applying finite solid-angle corrections, we find an anisotropy of $A = 0.106 \pm 0.011$. The correction due to the finite source extension amounts to an increase of this value by less than 0.003 [ based on the formula (3) in Ref. 5]. A decrease of the measured anisotropy due to Compton scattering of the 55-keV $\gamma$ rays in the wall of the source ampoule was estimated and found negligible. As the final result we adopt the value listed in Table I.

All the present knowledge of anisotropies of $\gamma$-$\gamma$ directional correlations measured with low-density gaseous sources of $^{127}$Xe and $^{125}$Xe is summarized in Table I. The anisotropy of the 172–203-keV cascade has recently been remeasured.[8] Both our values agree with each other

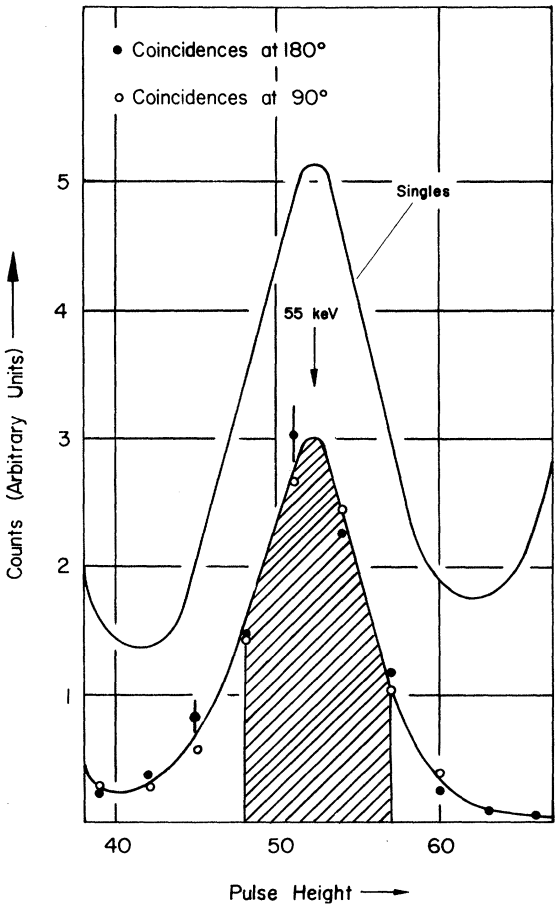


FIG. 4. Singles and coincidence spectra in fixed detector around 55 keV with single channel of movable detector at 188 keV. Single-channel positions for anisotropy measurement are indicated.

but disagree with the value reported by Jha and Leonhard.[9] This discrepancy could be understood if the pressure in the source of Jha and Leonhard would have been larger than 1 Torr (see Refs. 8 and 10).

The results listed in Table I clearly demonstrate that the angular correlations are strongly perturbed. The perturbation must be due to the hyperfine interaction of the radioactive ions. A more quantitative discussion of these results can be found in Sec. III of the following paper[11] (henceforth referred to as II).

## IV. RESONANCE EXPERIMENT

Theoretically, one expects to find resonances in perturbed (time-integrated) angular correlations if the following conditions are fulfilled.[12–14] (i) The interaction between the nucleus and its surroundings is strong, i.e., the energy splittings of the nuclear system in the intermediate state are large compared to the natural width $\Gamma$. (ii) The interaction is "time independent," i.e., the nuclear surroundings remain unchanged during the lifetime of the intermediate nuclear state. (iii) Two or more levels cross for some particular value of an externally controllable parameter, such as an applied magnetic field. (iv) The states corresponding to the crossing levels are capable of interference.[15,16]

It has been shown that in the case of an angular correlation perturbed by the hyperfine interaction of a free atom or ion a resonance should occur around zero magnetic field.[3] The complete theory of this effect has been worked out in Ref. 17. Here, we quote the result for observation of the $\gamma$ rays perpendicular to the applied magnetic field $H$, and for directional correlations having no $A_4$ term

$$W(\Phi)=D_0+\sum_F D_{F2}\frac{\cos 2\Phi-2\gamma_F X\sin 2\Phi}{1+4\gamma_F^2X^2}\ , \quad (1)$$

where $\Phi$ is the angle between the directions of the two $\gamma$ rays, and the magnetic field parameter $X$ is given by

$$X=g_J\mu_B H/\Gamma\ . \quad (2)$$

Here $g_J$ is the splitting factor of the atomic state (total angular momentum $J$), and

$$\gamma_F=[F(F+1)+J(J+1)-I(I+1)]/2F(F+1) \quad (3)$$

is the ratio between the splitting factor of a state with total angular momentum $F$ and $g_J$. The nuclear spin $\vec{I}$ of the intermediate state is coupled with the atomic spin $\vec{J}$ to form a system with total angular momentum

$$\vec{F}=\vec{I}+\vec{J}\ . \quad (4)$$

The quantities $D_0$ and $D_{F2}$ in Eq. (1) depend on the $A_2$ coefficient of the unperturbed angular correlation and on angular momentum quantum numbers

$$D_0=1+\tfrac{1}{4}A_2\sum_F\frac{(2F+1)^2}{2J+1}\begin{Bmatrix}FF2\\IIJ\end{Bmatrix}^2\ , \quad (5)$$

$$D_{F2}=\tfrac{3}{4}A_2\frac{(2F+1)^2}{2J+1}\begin{Bmatrix}FF2\\IIJ\end{Bmatrix}^2\ . \quad (6)$$

In this section, we describe the angular-correlation experiment performed on the cascade of 172–203 keV that led to the observation of the resonance effect. According to Eq. (1), the resonance line is a sum of Lorentzian-shaped curves if the $\gamma$ rays are measured at angles $\Phi=\pi$ and $\Phi=\frac{1}{2}\pi$, respectively. In order to be largely independent of possible magnetic field effects on the detectors, we have measured at two angles, and we have determined the anisotropy function

$$A(H)=[W(\pi)-W(\tfrac{1}{2}\pi)]/W(\tfrac{1}{2}\pi)\ . \quad (7)$$

Possible scattering effects from materials close to the source (e.g., from the pole pieces) are avoided by measuring also $A(0)$ in the presence of the magnet. The difference $A(0)-A(H)$ is then the quantity that has to be compared to the theoretical expression. The true value $A(0)$ may be obtained from the separate measurement described in Sec. III A. The 203-keV $\gamma$ ray was measured with the movable detector which consisted of a $1\frac{3}{4}\times\frac{1}{2}$-in. NaI (Tl) crystal mounted on a 12-in.-long light-pipe. The front end of the crystal was placed $1\frac{1}{2}$ in. from the center of the source. A heavy multilayer magnetic shielding cylinder was placed around the phototube, extending considerably beyond the photocathode. In addition, two $\frac{3}{8}$-in.-thick iron plates were mounted perpendicular to the detector axis at a position about half-way between the shielding cylinder and the NaI crystal. The fixed detector was a $3\times 3$-in. Harshaw integral-line unit surrounded by a heavy magnetic shielding cylinder which was constructed with different magnetic materials. The shielding cylinder extended up to the front face of the detector. Its front end was closed with two sheets of 0.33-g/cm$^2$ Armco iron in order to prevent the magnetic field from entering the shielding cylinder along the axis. The front end of the detector was placed at a distance of 5 in. from the source for large values of the magnetic field, and a distance of 4 in. was used for small magnetic fields. The magnetic field was produced with a $C$-type electromagnet having an air gap of $1\frac{1}{2}$ in. The field was measured to 1% accuracy with a rotating-coil gaussmeter. The homogeneity of the field in the region occupied by the source was found to be better than 2%. Most measurements were carried out with the source described in Sec. III A (source

strength approximatively 10 $\mu$Ci). Magnetic field or angular position was changed every 10 min. The results are shown in Fig. 5 (circular points). Some preliminary measurements were performed with a source having a 18 mm diam and a pressure of about 1.5 Torr (triangular points in Fig. 5). Magnetic field effects on both detectors were carefully checked. The change in pulse height of the fixed detector was always less than 0.2% for fields $|H| \leq 1$ kG. The movable detector did show pulse-height changes up to 0.6% at $H = 1$ kG. The difference in the pulse-height changes for the two angular positions $\Phi = \pi$, $\frac{1}{2}\pi$, however, was always smaller than 0.2%. On the basis of the single-channel window positions used in the experiment, we estimate possible effects on the measured quantity $A'(0) - A'(H)$ to be less than 0.002 which is much smaller than the statistical uncertainties indicated in Fig. 5. At the largest fields studied, $H = \pm 1.69$ kG, small magnetic field effects on the fixed detector were seen. We have attempted to correct for them by using the singles counting rate measured simultaneously. In view of possible remaining uncertainties the corresponding values have not been used in the analysis of the data. A further direct test on the absence of magnetic field effects on the detector system was carried out by measuring the same angular correlation in a metallic source. In this case, no (or at most a very weak) resonance effect should exist. The aluminum foil source of $^{127}$Xe described in an earlier work[5] has been used. The result obtained (rectangular point in Fig. 5) demonstrates the absence of magnetic field effects on the detectors.

The data of Fig. 5 were analyzed by fitting a single Lorentzian curve to the circular points with $|H| \leq 1$ kG. The least-squares fit gave a value for the half-width at half-maximum of the resonance of

$$\Delta H = 195 \pm 41 \text{ G}. \tag{8}$$

According to Eqs. (1) and (2), this value is a measure of the Zeeman splitting of the hyperfine levels in units of the natural width $\Gamma$ and is independent of finite solid-angle effects for a point source (see Appendix). Corrections for the finite source extension are believed to be small.[18] The least-squares fit yields also a value for the height of the resonance $A(0) - A(\infty)$ (corrected for finite solid angles according to the procedure described in the Appendix):

$$A(0) - A(\infty) = 0.045 \pm 0.004. \tag{9}$$

A measurement of the resonance line at an angle $\Phi = \frac{3}{4}\pi$ is sensitive to the sign of $g_J$ [see Eq. (1)]. We have measured at a fixed angle $\Phi = \frac{3}{4}\pi$ the coincidence counting rate with a positive magnetic field $W_+(\frac{3}{4}\pi)$, and also with reversed magnetic field $[W_-(\frac{3}{4}\pi)]$. In Fig. 6, the quantity $[W_+(\frac{3}{4}\pi) - W_-(\frac{3}{4}\pi)]/W_-(\frac{3}{4}\pi)$ is plotted as a function of the magnetic field $|H|$. The dashed curve in Fig. 6 represents the function

$$f(H) = [A(0) - A(\infty)] \frac{H/\Delta H^2}{1 + (H/\Delta H)^2}, \tag{10}$$

where $A(0) - A(\infty)$ and $\Delta H$ have been assumed to be the measured values (9) and (8), respectively.

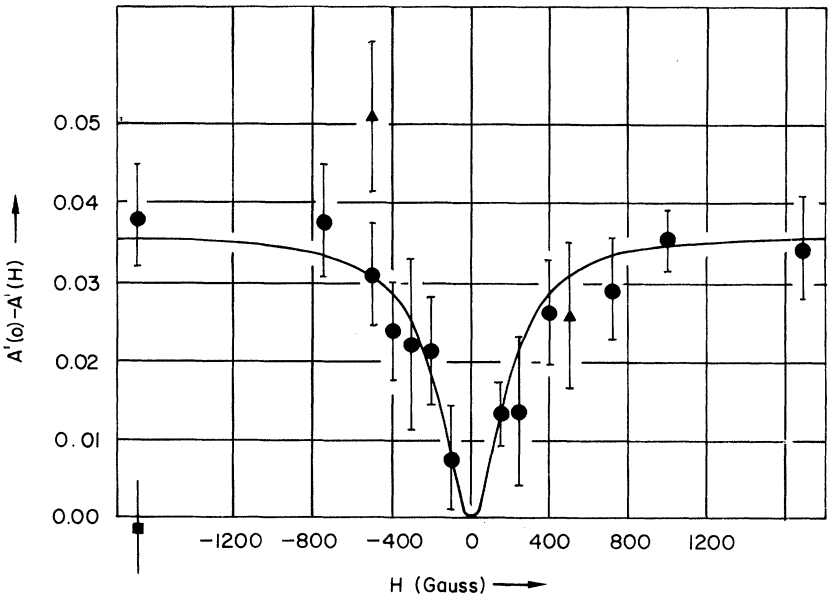


FIG. 5. Anisotropy at zero field minus anisotropy at field $H$, measured as a function of $H$. (Uncorrected for solid-angle effects.) Circular points, source described in Sec. III A; triangular points, source with diameter 18 mm; rectangular point, metallic source.

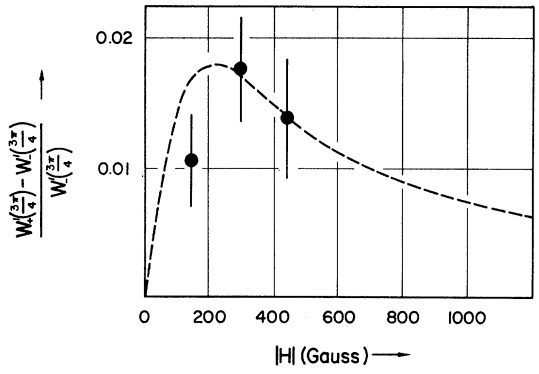


FIG. 6. Difference of coincidence counting rates with positive field ($W'_+(\frac{3}{4}\pi)$) divided by $W'_-(\frac{3}{4}\pi)$, plotted as a function of the field $|H|$. (Uncorrected for solid-angle effects.)

The measured sign of the quantity plotted in Fig. 6 implies a positive sign of $g_J$ (see discussion in Ref. 2, Sec. III).

Further implications of the parameters deduced from the resonance experiment may be found in Sec. III of Ref. 2. There, the hyperfine effects observed in angular correlations are related to the various phenomena that occur in the atom, as a consequence of a preceding electron-capture process.

## APPENDIX: FINITE SOLID-ANGLE CORRECTIONS FOR RESONANCE EXPERIMENTS

The angular correlation function equation (1) is valid for an ideal geometry, i.e., for a point source and a detector system defining narrow emission directions of the $\gamma$ rays. In practice, the more important corrections arise from the finite solid angles of the detectors. In this section, we discuss the effects of finite solid angles on resonance experiments assuming a point source and detectors that are rotationally symmetric. The efficiency of the detectors may still depend on the direction of the incident $\gamma$ ray with respect to the symmetry axis of the detector.

A time-integrated angular correlation that is perturbed by a stationary (but otherwise arbitrary) extranuclear field may always be written[14]

$$W = \sum_{b,b'} \frac{F_{bb'}(1) F_{bb'}(2)}{1 - i[(E_b - E_{b'})/\Gamma]} \quad , \tag{11}$$

where $|b\rangle$ is an energy eigenstate of the total system when the nucleus is in its intermediate state, and $E_b$ is the corresponding energy. The quantities $F_{bb'}(1)$ and $F_{bb'}(2)$ may be expressed

$$F_{bb'}(1) = \sum_{k_1\mu_1} A_{k_1}(1)\, S_{bb'}(k_1\mu_1)\, Y_{k_1\mu_1}(\vartheta_1, \varphi_1) \, ,$$

$$F_{bb'}(2) = \sum_{k_2\mu_2} A_{k_2}(2) S^*_{bb'}(k_2\mu_2)\, Y^*_{k_2\mu_2}(\varphi_2, \varphi_2), \tag{12}$$

where $A_k(1)$ and $A_k(2)$ are the usual coefficients describing the unperturbed angular correlation,[19] the quantities $S_{bb'}(k\mu)$ depend on the properties of the states $|b\rangle$, and $Y_{k\mu}(\vartheta, \varphi)$ are spherical harmonics. The emission directions of the first and the second $\gamma$ rays are described in some space-fixed frame of reference by the angles $(\vartheta_1, \varphi_1)$ and $(\vartheta_2, \varphi_2)$, respectively. It follows then from Eqs. (12), that the angular dependence of the correlation function (11) is given by products of spherical harmonics. The effects of finite solid angles may be evaluated for each product term

$$Y_{k_1\mu_1}(\vartheta_1, \varphi_1)\, Y^*_{k_2\mu_2}(\vartheta_2, \varphi_2) \, . \tag{13}$$

We assume the detectors to be held at fixed positions. Integration over all directions of $\gamma$ rays that are accepted by the detectors transforms expression (13) into [20]

$$Q_{k_1}(1)\, Q_{k_2}(2)\, Y_{k_1\mu_1}(\bar{\vartheta}_1, \bar{\varphi}_1)\, Y^*_{k_2\mu_2}(\bar{\vartheta}_2, \bar{\varphi}_2) \, , \tag{14}$$

where $(\bar{\vartheta}_1, \bar{\varphi}_1)$ and $(\bar{\vartheta}_2, \bar{\varphi}_2)$ are now the directions of the symmetry axes of the detectors measuring the first and the second $\gamma$ rays, respectively. The quantities $Q_k(1)$ and $Q_k(2)$ reflect the properties of the two detectors and have been calculated by Yates[20] for NaI (Tl) detectors and various geometries. (The normalization is such that $Q_0 = 1$.)

Application of expression (14) to the special case of the resonance treated in Sec. IV, combined with the derivation of the correlation function (Ref. 17) yields the following modifications of the theoretical results quoted in Sec. IV: (i) The angle $\Phi$ appearing in Eq. (1) has to be taken as the angle between the two detector axes. (ii) The coefficient $A_2$ in Eqs. (5) and (6) has to be replaced by $Q_2(1)Q_2(2)A_2$. This implies that the width of the resonance remains unchanged by finite solid-angle effects, while the height of the resonance is reduced by the factor $Q_2(1)Q_2(2)$.

*Work supported in part by the U. S. Atomic Energy Commission.

†Some results have previously been reported by H. J. Leisi, Phys. Letters 12, 221 (1964); 17, 308 (1965).

‡Present address.

[1]Effects on angular correlations have been reviewed by H. Frauenfelder and R. M. Steffen in *Alpha-, Beta- and Gamma-Ray Spectroscopy*, edited by K. Siegbahn, (North-Holland, Amsterdam, 1965), Vol. 2, Chap. XIXA, p. 1182. A compilation of Mössbauer effect work may be found in W. Triftshäuser and P. P. Craig, Phys. Rev. Letters 16, 1161 (1966). See also, P. Jung and W. Triftshäuser, Phys. Rev. 175, 512 (1968).

[2]*Perturbed Angular Correlations*, edited by E. Karlsson, E. Matthias, and K. Siegbahn (North-Holland, Amsterdam, 1964), p. 329.

[3]H. J. Leisi, in *Perturbed Angular Correlations*, edited by E. Karlson, E. Matthias, and K. Siegbahn (North-Holland, Amsterdam, 1964), p. 318.

[4]S. J. Balestrini, Phys. Rev. 95, 1502 (1954).

[5]H. J. Leisi, Nucl. Phys. 76, 308 (1966).

[6]M. J. L. Yates, in *Alpha-, Beta-, and Gamma-Ray Spectroscopy*, edited by K. Siegbahn (North-Holland, Amsterdam, 1965), Vol. 2, Appendix 9.

[7]This value is slightly different from the value quoted in H. J. Leisi, Phys. Letters 17, 308 (1965) as a result of a more thorough evaluation of the data.

[8]F. N. Gygax, J. Egger, and H. J. Leisi, in *Hyperfine Structure and Nuclear Radiations*, edited by E. Matthias and D. A. Shirley (North-Holland, Amsterdam, 1968), p. 948.

[9]S. Jha and R. Leonhard, Phys. Rev. 136, B1585 (1964).

[10]F. N. Gygax, J. Egger, and H. J. Leisi, in *Proceedings of the Conference on Electron Capture and Higher-Order Processes in Nuclear Decays, Debrecen, Hungary, July* 15-18, 1968, edited by D. Berényi (Eötvös Lorànd Physical Society, Budapest, 1968), p. 386.

[11]H. J. Leisi, following paper, Phys. Rev. A 1, 1662 (1970).

[12]H. J. Leisi and R. T. Deck, Phys. Rev. 129, 2117 (1963); 131, 2840 (E) (1963).

[13]M. I. Podgoretskii and O. A. Khrustalev, Usp. Fiz. Nauk 81, 217 (1963) [Soviet Phys. Usp. 6, 682 (1964)].

[14]H. J. Leisi, Habilitationsschrift, Swiss Federal Institute of Technology, 1967 (unpublished).

[15]H. J. Leisi, in *Hyperfine Structure and Nuclear Radiations*, edited by E. Matthias and D. A. Shirley (North-Holland, Amsterdam, 1968), p. 379.

[16]Reference 15, p. 397.

[17]Reference 15, p. 384.

[18]See formula (3) in Ref. 5.

[19]See, e.g., in *Alpha-, Beta- and Gamma-Ray Spectroscopy*, edited by K. Siegbahn (North-Holland, Amsterdam, 1965), Appendix 8.

[20]Reference 6, Appendix 9.